*Send Orders for Reprints to reprints@benthamscience.ae*

*Current Pharmaceutical Biotechnology*, 2015, *16*, 000-000 

# Synthesis and Characterization of Ibandronate-Loaded Silica Nanoparticles and Collagen Nanocomposites

G.S. Alvarez, M.I, Alvarez Echazú, C. E. Olivetti and Martín F. Desimone*

*IQUIMEFA-CONICET. Facultad de Farmacia y Bioquímica, Universidad de Buenos Aires, Junín 956, Piso 3° (1113), Buenos Aires, Argentina*

**M.F. Desimone**

**Abstract:** Non-porous bare silica nanoparticles, amine modified silica nanoparticles and mesoporous particles, were evaluated as carriers for sodium ibandronate. The synthesized nanoparticles were characterized by SEM, TEM, DLS and porosity. Then, their capacity to incorporate a bisphosphonate drug (sodium ibandronate) and the *in vitro* release behavior was analyzed by capillary electrophoresis. Mesoporous and amine-modified particles showed higher levels of drug incorporation, 44.68 mg $g^{-1}$ and 28.90 mg $g^{-1}$, respectively. The release kinetics from the two types of particles was similar following a first order kinetics. However, when these particles were included into collagen hydrogels only mesoporous nanoparticles had a sustained release for over 10 days. The biocompatibility of mesoporous particles towards Saos-2 cells was also evaluated by the MTT assay observing an increase in cell viability for concentrations lower than 0.6 mg $ml^{-1}$ of particles and a decrease for concentrations over 1.2 mg $ml^{-1}$. Furthermore, when these particles were incubated with mesenchymal cells it was observed that they had the capacity to promote the differentiation of the cells with a significant increase in the alkaline phosphatase activity.

**Keywords:** Collagen, ibandronate, silica, nanoparticles.

## INTRODUCTION

Initially, bisphosphonates (BPs) were shown to have a high affinity for bone hydroxyapatite and to inhibit the dissolution of calcium phosphate crystals *in vitro* [1]. Later it was found that as well as this physicochemical effect they inhibit bone resorption *in vivo*. The pharmacological effect of bisphosphonates is then related to both their binding to bone mineral phases and their biochemical effect on cells, predominantly osteoclasts [2]. Bisphosphonates have two main mechanisms of inhibition towards osteoclasts depending on the characteristics of the drug. In the case of first-generation bisphosphonates, which do not contain nitrogen atoms in their structure, they act as analogs of pyrophosphates and they are metabolized to a cytotoxic analog of ATP [3] while the second generation bisphosphonates, like sodium ibandronate, inhibit the farnesyl pyrophosphate synthase reducing the amount of farnesyl diphosphate (FPP) and geranylgeranyldiphosphate (GGPP) required for protein prenylation [4]. When prenylation is inhibited, the osteclast activity decreases leading to apoptosis [5].

These drugs are recommended for clinical use in Paget's disease, hypercalcemia, and osteoporosis. The oral route is the most preferred for chronic drug therapy. However its major disadvantage is their poor absorption (less than 1% of the oral dose) in the gastrointestinal tract. The i.v administration of BPs is an alternative route where approximately 30-80% of the dose is excreted into the urine, and most of the rest is bound to the bone remaining for long periods of time [6].

Apart from the systemical administration of these drugs, local application of BPs has gained attention in recent years due to advantages such as reduced adverse effects and high local concentration. This fact led to the development of different local delivery systems like coatings [7], nanoparticles [8, 9], hydrogels or nanocomposites [10-11]. As an example, chitosan and poly(lactide-co-glycolide) acid (PLGA) microspheres loaded with alendronate were prepared for orthopedic as well as dental applications. It was observed that 85% of the drug had been released at the end of the third day from chitosan microspheres whereas 58% was released at the end of the fifth day from PLGA microspheres [12]. In the same way, some *in vivo* experiments have been performed where zoledronate locally delivered from a cross-linked hyaluronic acid hydrogel boosted bone formation rate up to 100% during the first 17 days after implantation and reduced the bone resoption rate in a ovariectomized rat femoral model [13]. Furthermore, zoledronate was also grafted to hydroxyapatite coatings of titanium implants and these implants were inserted in rat condyles showing a positive effect on the peri-implant bone density and an increased mechanical fixation [14].

Besides their antiresorptive function, BPs can also be locally used with other purposes. In this sense, a poly (2-hydroxy methacrylate) hydrogel was functionalized with alendronate for the treatment of chronic wounds. The com-

*Address correspondence to this author at the IQUIMEFA-CONICET. Facultad de Farmacia y Bioquímica, Universidad de Buenos Aires, Junín 956, Piso 3° (1113), Buenos Aires, Argentina; Tel: +54-1149648254; Fax: +54-1149648254; E-mail: desimone@ffyb.uba.ar

In memoriam of Prof. Dr. Luis E Diaz.

1389-2010/15 $58.00+.00 

mon pathology in these chronic wounds is excessive proteolytic activity, resulting in degradation of key factors critical to the ulcer's ability to heal. As matrix metalloproteinases are zinc-dependent endopeptidases that show an increased activity in chronic wound fluid, the authors probed that their activity could be inhibited with the bisphosphonate alendronate which is capable of binding to divalent metal like $Zn^{2+}$ [15]. Considering the selection of the most appropriate constituents of these hydrogels, a possible challenging approach is the 'biomimetic' one where the prepared biomaterial should resemble the tissue to be repaired as closely as possible [16-21]. An example is provided by recent efforts to build up bone-like materials from collagen [22]. In this sense, silicified matrices exhibit increment in the rheological properties, enzymatic digestion occurred at a slower rate and cells seeded on silicified collagen matrices were able to adhere, proliferate and migrate within the scaffold [23-26]. In addition, silica nanoparticles have gained ground in the biomedical field for their biocompatibility and biodegradability, being themselves inert and stable, thus enabling a variety of formulation designs for application in the pharmaceutical industry [27-30].

The objective of the present work was to evaluate nonporous bare silica nanoparticles, amine modified silica nanoparticles and mesoporous silica nanoparticles as carriers for sodium ibandronate. Secondly, these particles were incorporated in collagen hydrogels in order to develop a new local delivery system. The release of ibandronate from the particles or from the Np-collagen nanocomposites was presented and compared. Cellular toxicity of Nps on osteoblast-like cells SAOS-2 was also performed using MTT assay and the effect on mesenchymal cells differentiation was assessed by measuring the alkaline phosphatase activity.

## MATERIALS AND METHODS

### Nanoparticle Synthesis

Three different types of silica nanoparticles were synthesized. Solid silica nanoparticles were obtained by Stöber method [31]. Briefly, tetraethyl orthosilicate (TEOS) was added to a stirred solution of ammonium hydroxyde (30 %) in a water/ethanol mixture to obtain silica nanoparticles. Solutions were stirred for 24 hours at room temperature and the resulting nanoparticles were recovered by centrifugation and washed with water until neutral pH was reached. Silica nanoparticle concentration was determined by weighting the residual mass of an aliquot dried at 80°C.

Amino-modified silica nanoparticles were obtained using the Stöber method described above but aminopropyltriethoxysilane (APTES) and TEOS were added simultaneously to the ammonium hydroxyde solution in a proportion 1:4.

Mesoporous silica Np were synthesized adding 5.0 g ethanol (108.70 mmol), 1.4 g aqueous ammonia (20.59 mmol) and 0.21 g cetyl trimethylammonium bromide (CTAB) (0.58 mmol) into 3.85 mL water (213.89 mmol) under stirring. After 15 min of stirring, 0.39 g of TEOS (1.88 mmol) was added dropwise into the above solution. The solution was continuingly stirred for 4 h. CTAB was removed by microwave digestion (MLS 1200 Mega, Milestone, Bergamo, Italy) in a $HNO_3$:$H_2O_2$ mixture (9:1 v/v). The synthesized Nps were centrifuged, washed with ethanol and water, and then dried under vacuum [32].

### Nanoparticle Characterization: Surface Area, Morphology and Size Distribution

The specific surface area, total pore volume, and pore size were measured for silica nanoparticles by nitrogen sorption at 77 K using an automatic gas adsorption analyzer (Gemini 2360 V2.00). Prior to the measurement, the nanoparticles powder was degassed for 24 h at 150ºC. The specific surface area was calculated according to the Brenauer–Emmett–Teller (BET) theory [33], while the pore size distribution and the total pore volume were calculated by the Barrett-Joyner-Halenda (BJH) method [34].

The shape and appearance were evaluated by scanning electron microscopy (SEM) and transmission electron microscopy (TEM). The nanoparticles were analyzed using a Zeiss Supra 40 microscope for SEM. Samples for SEM analysis were prepared by gold-sputtering the nanoparticles in an argon atmosphere.

Particle size analysis and zeta potential was performed by the light diffraction method. The samples were suspended in filtered 10mM KCl, sonicated for 30 seconds, and subsequently analyzed. Triplicate analyses were performed for each sample of nanoparticles.

### Adsorption Isotherms for Silica Nps with Sodium Ibandronate Solutions

Ibandronate adsorption experiments were carried out by a batch method at room temperature (25ºC). The three types of silica nanoparticles obtained (20 mg) were put in contact with 1 ml of sodium Ibandronate solutions ranging from 7.5 to 0.1 g $L^{-1}$. Adsorption isotherms were determined by monitoring the drug in the supernatant solution. The method employed to evaluate the concentration of sodium ibandronate in the solutions was capillary electrophoresis (CE).

### Capillary Electrophoresis Method

Electrophoresis was carried out on an Agilent capillary electrophoresis system with diode array detector (Agilent Technologies). Capillary electrophoresis analyses were performed using uncoated fused-silica capillary column (Polimicro Technologies, Phoenix, Arizona, USA) of 50 µm internal diameter and 50 cm total length (40 cm to detector).

The background electrolyte (BGE) consisted of a 7.5 mM Phtalic acid solution pH 3.5. BGE solution was filtered through 0.45µm syringe filter and sonicated (Transsonic 540 sonicator, 35kHz; Elma, Singen, Germany) before used. The voltage applied was -30kV. For sample introduction, positive pressure was applied (500 mbar.s). Indirect on-line UV detection was achieved at 205nm [35]. For capillary conditioning, new capillaries were flushed with water for 5 min, sodium hydroxide 0.5 M for 10 min, water for 5 min and finally BGE for 10 min. between each run, the capillary was flushed with BGE for 2 min.

A 1000 µg $ml^{-1}$solution of sodium ibandronate was prepared in water to build a standard curve in the range 1 to 100 µg $ml^{-1}$. Samples were obtained from the supernatant of

MNP or collagen composites incubated in water (as indicated in the adsorption and release experiments section) and injected after centrifugation. All experiments and measurements were conducted in triplicate.

### Determination of *in vitro* Drug Release Profiles of Ibandronate-Loaded Nanoparticles

The rates of ibandronate release from nanoparticles were evaluated in water at 37ºC. Briefly, 60 mg of drug-loaded nanoparticles were added to 5 ml of water and the mixture was sonicated for 20 sec to disperse the particles. The nanoparticle suspension was then placed on a rotary shaker set at a speed of 100 rpm/min. The liquid medium was completely replaced with fresh water at various intervals prior centrifugation to separate the nanoparticles from the solution. The amount of ibandronate released to the supernatant was measured by capillary electrophoresis according to the method described above.

### Synthesis and Characterization of Silica Np-collagen Nanocomposites

Collagen type I was purified from rat tails and the concentration was estimated by hydroxyproline titration. Nanocomposites were prepared by mixing a 5.0 mg $mL^{-1}$ collagen suspension in 17 mM acetic acid solution with a suspension containing a 0,25M of drug-loaded silica nanoparticles (15 mg per gel). The resulting sols were dispatched into 24-well plates and let for 2 hs under ammonia vapors. Finally, they were afterwards let under extraction for the ammonia to evaporate until they reached pH 7.

Scanning electron microscopy (SEM) analysis was performed to the nanocomposites. Collagen nanocomposites were fixed using 3.63% glutaraldehyde in a cacodylate/ saccharose buffer (0.05 M/0.3 M, pH 7.4) for 1 hour at 4ºC. Following fixation, samples were washed three times with the same buffer and dehydrated through successive increasing concentration ethanol baths from 70% to 100% alcohol. Thereafter, samples were dried in a critical point dryer and gold sputtered (10 nm) for analysis [36]. Samples were observed with a Zeiss Supra 40 microscope for Scanning Electron Microscopy (SEM).

Drug release experiments were also performed to the nanocomposites. For this purpose, each gel was let with 1.25 ml of water on a rotary shaker at a speed of 100 rpm $min^{-1}$. The liquid medium was completely replaced with fresh water at various intervals.

### Cell Culture and *in vitro* Toxicity Experiments

The SAOS-2 cell line (osteogenic sarcoma) was grown in adherent culture flasks in DMEM (Sigma) supplemented with 10% heat-inactivated fetal calf serum and 1% Penicillin-Streptomycin. Cells were kept at 37ºC in a humidified 5% carbon dioxide chamber until confluence was reached. Harvesting was done with a trypsin-EDTA solution following the protocol provided by the manufacturer. Before each use cells were stained with trypan blue and counted in a Neubauer camera.

For toxicity experiments, cells were seeded ($1x10^4$ per well) and silica nanoparticle suspensions were added with concentrations ranging from 0.06 to 2.4 mg $mL^{-1}$ followed by addition of 1 mL DMEM. After a 2-day culture period, cell metabolic activity was measured using the MTT assay. For that purpose the medium was removed, replaced with 0.45 ml of fresh media and 0.05 ml of a 5 mg $mL^{-1}$ MTT solution and incubated in a humidified 5% carbon dioxide chamber for 4 h. Following incubation, MTT solution was removed and 1 ml of absolute ethanol was added. The absorbance was recorded at 570 nm [25]. In all cases results are expressed as mean $\pm$ SD from triplicate experiments.

### Mesenchymal Cells Differentiation

Osteoblasts show high alkaline phosphatase (AP) activity, therefore the activity of this enzyme is a feasible marker for cell differentiation. Mesenchymal cells were obtained from femoral bone marrow of rats according to the protocol Isolation of Rat MSCs [37] and they were cultured in αMEM media. Afterwards, cells were trypsinized and plated into 24-well culture dishes (4 replicates for detection of the alkaline phosphatase activity) at a concentration of 1.000 cells per well in 1 ml medium. After confluence, the different media were added and renewed every two days. For positive control αMEM media was complemented with 20 mM β-glycerophosphate, 100 nM dexamethasone and 50 μM ascorbic acid.

Mesoporous nanoparticles were added to the culture media in concentrations of 0,36 μg $L^{-1}$ and 3,6 μg $L^{-1}$ which, in same experiments, were also loaded with sodium ibandronate in concentrations around $10^{-8}$ M and $10^{-7}$ M, respectively. In another case, αMEM media was also prepared by the addition of $10^{-8}$ M sodium ibandronate without particles.

The cells were washed and lysed after 5, 10 and 15 days with 400 μl of a buffer containing 0,1M diethylamine (DEA), 1 mM $MgCl_2$ and 0.1% Triton X-100 by two freeze-and-thaw cycles.

Alkaline phosphatase activity was determined with *p*-nitrophenylphosphate as the substrate. 50 μl of samples were added to 100 μl *p*-nitrophenylphosphate (5 mM) in the same buffer used for lysis and incubated at 37°C for 60 min on a shaker. The enzymatic reaction was stopped by adding 20 μl of 1 M NaOH. Enzyme activity was quantified by absorbance measurements at 405 nm and calculated according to a series of *p*-nitrophenol standards.

### Statistical Analysis

All experiments were performed in triplicate and statistically analyzed by one-way ANOVA. Data are represented as means + SE. The differences were analyzed using one way ANOVA, followed by Bonferroni's Multiple Comparison Test, when $p < 0.05$ difference was considered significant.

## RESULTS AND DISCUSSION

### Particle Characterization

Three types of silica nanoparticles were obtained. Solid silica nanoparticles (SNp) had a mean diameter of 656.5±94.1 nm. Particle size analysis using DLS also revealed a homogeneous distribution confirmed by TEM imaging as well as the absence of significant aggregation (Fig. **1a**). When these

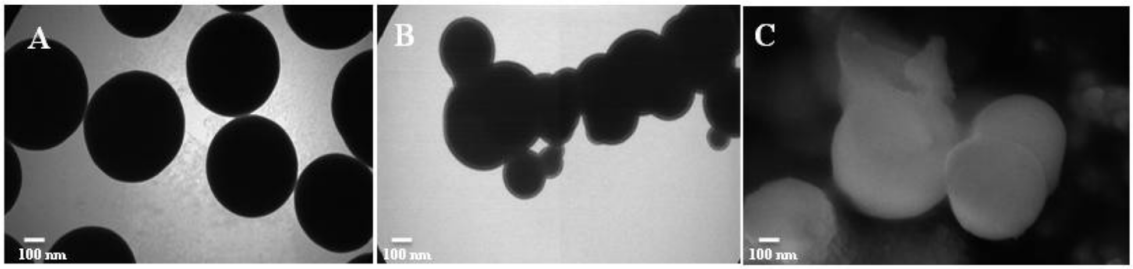


**Fig. (1).** TEM and SEM images of silica nanoparticles. **a**) TEM for solid nanoparticles **b**) TEM for MNP **c**) SEM for MNP.

particles were modified by the addition of APTES, the zeta potential ζ changed from -42mV to +19mV showing the successful incorporation of amine groups to the surface of the particles. The measured DLS particle size for them was 630.0±48.9 nm, similar to the one obtained for SNps. The particle size observed for the mesoporous nanoparticles (MNP) had a mean diameter of 532.9±35 as it can be seen in TEM and SEM images (Fig. **1b** and **c**).

BET measurements revealed for the MNP a specific surface area of as high as 596.9 $m^2g^{-1}$ and a total pore volume of 0.331 ml $g^{-1}$ with a porous radio of 1.25 nm. In the case of solid nanoparticles the specific surface area was around 17.4 $m^2g^{-1}$ confirming the absence of porosity.

### Incorporation of Sodium Ibandronate into Nanoparticles and *in vitro* Drug Release

Adsorption isotherms are presented for amine-modified and mesoporous particles (Fig. **2**). Langmuir isotherms were modeled in order to characterize the interaction of the drug with the silica nanoparticles. Langmuir isotherms can be expressed as follows:

$$q = qoCeq/K + Ceq$$

where q is the adsorption capacity expressed as the amount of adsorbed drug per mass unit of nanoparticles (mg $g^{-1}$), K is the adsorption equilibrium constant (mg $ml^{-1}$), qo is the maximal adsorption capacity (mg $g^{-1}$) and Ceq is the equilibrium concentration of the incubation solution.

Sodium ibandronate pKa is 2.0, 6.3 and 10.5 with a negative charge at physiological pH. This fact can explain why the loading of solid silica nanoparticles with a negative zeta potential is very low (less than 1 mg $g^{-1}$) compared to amine-modified silica nanoparticles which can incorporate as much as 28.90 ± 3,13 mg $g^{-1}$ of Np. In this case, the main mechanism of drug incorporation might be an electrostatic interaction between the negatively charged drug and the positive surface of non-porous particles. For MNP the drug loading was even higher, with a maximum capacity of 44.68 ± 4,86 mg $g^{-1}$ which cannot be explained through electrostatic interaction because they are also negatively charged, but in terms of high surface area. As MNP have high porosity the drug can be entrapped within those pores.

As shown in (Fig. **3**), drug release from the two types of particles is similar following a first order kinetics and only slightly slower for MNPs. In both cases a rapid burst release was observed, reaching almost 50% after 5 hs and 100% after 2 days of incubation.

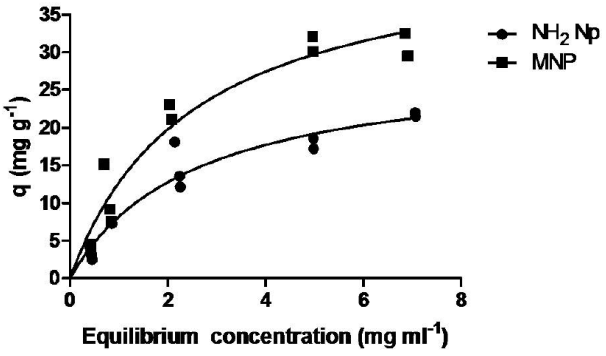


**Fig. (2).** Adsorption isotherms of sodium ibandronate for amine-modified nanoparticles ($NH_2$ Np) and mesoporous silica nanoparticles (MNP).

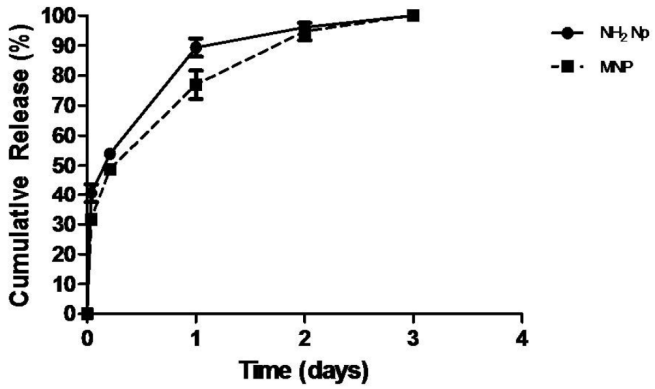


**Fig. (3).** Cumulative *in vitro* release from amine-modified ($NH_2$ NP) and MNP loaded with sodium ibandronate.

### Synthesis and Characterization of Nanocomposites*: in vitro* Release

SEM images showed a typical dense fibrillar collagen network with high porosity when collagen hydrogels were prepared without the addition of nanoparticles (Fig. **4A**) which was not altered after the incorporation of MNP loaded with sodium ibandronate (Fig. **4B**).

When these nanoparticles were included in collagen hydrogels to prepare nanocomposites, it was observed (Fig. **5**) that pure collagen gels used as a control and nanocomposites with amine- modified particles also had a fast release, reaching almost a 90% in the first two days. However, nanocomposites made of collagen and MNP showed a more sustained

release pattern, 60% of the drug was released after 2 days and after that the release was sustained for a period of 10 days. It is worth mentioning that in the case of amine-modified particles the drug is only included in the surface of the particle as they have no porosity. On the other hand, MNP have a high surface area that allows the drug to be dispersed in the whole particle. In this material that retains its shape the release of the drugs is by diffusion. Thus, the liquid needs to penetrate within the collagen polymer in the first step and then has to enter the pores of MNP to enable the drug to diffuse into the external media.

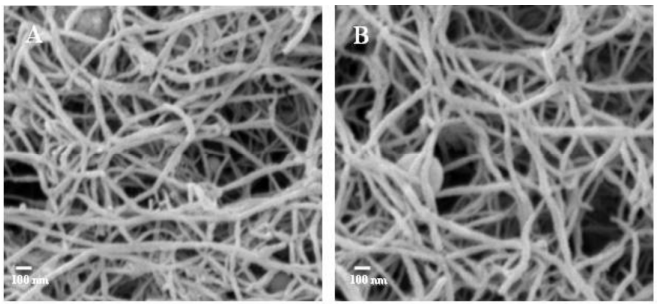


**Fig. (4).** SEM images of pure collagen hydrogels (**A**) and silica MNP-collagen composites (**B**).

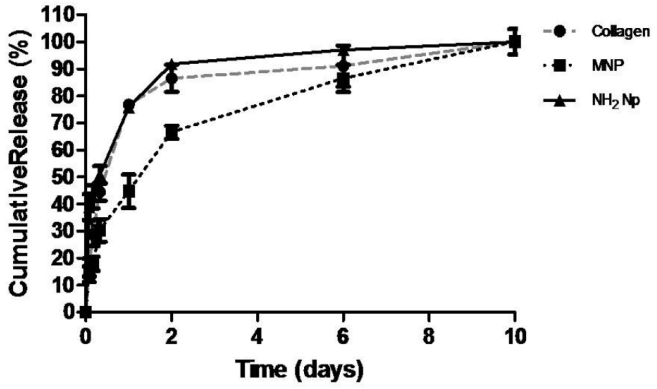


**Fig. (5).** Cumulative *in vitro* release of sodium ibandronate from silica-collagen composites.

Recently, it was found that silica particles carrying the antibiotic gentamycin could be immobilized at high silica dose in concentrated collagen hydrogels without modifying their fibrillar structure or impacting on their rheological behavior and increasing their proteolytic stability and mechanical stability. At the same time, gentamicin release from the nanocomposites was sustained over 7 days in comparison to free particles [27, 36].

### Toxicity Assay and Mesenchymal Cell Differentiation

As MNP had a higher maximum capacity of incorporating the drug and a better and slower sustained release when included into collagen hydrogels, it was decided to only performed cell experiments with this type of silica Np. Therefore, the effect of various mesoporous silica nanoparticle concentrations on SAOS viability was determined *in vitro*. These nanoparticles (without drug) significantly increased cell proliferation after 48 h compared to a control in concentrations between 0.06 and 0.6 mg $ml^{-1}$. However, nanoparticles in concentrations above 1.2 mg $ml^{-1}$ appeared to be toxic for cell with a 40 % decrease in their viability for 2.4 mg $ml^{-1}$ (Fig. **6**). These results are in agreement with previous works where rat primary culture osteoblasts in contact with the ionic products from the dissolution of a bioactive glass with 60% of silica, increased their viability when compared to control cultures [38].

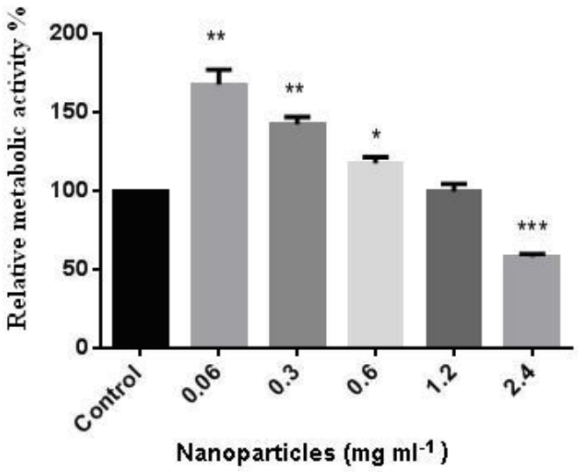


**Fig. (6).** Cytotoxicity of MNP in different concentrations for SAOS cells after 2 days of exposure performed by the MTT assay represented as percentage of viability with respect to a control group. * Indicates a statistical significance compared to the control group.

Alkaline phosphatase activity was measured after incubating mesenchymal cells with MNP loaded or not with sodium ibandronate. It could be observed (Fig. **7**) that sodium ibandronate ($10^{-8}$ M) had a positive effect on cell differentiation as ALP activity significantly increased after 5 and 10 days of culture in comparison with the negative control, in agreement with was previously reported for the same concentration of other bisphosphonates [39]. Von Knoch *et al*., demonstrated that zoledronate, risedronate and alendronate promote osteoblast differentiation of bone marrow stem cells, providing further evidence of their anabolic effects on osteoblasts [40]. In the same way nanoparticles carrying the drug in two different concentrations ($10^{-8}$ and $10^{-7}$) produced an increased in the ALP activity after 10 days of culture probably due to the fact that the drug release is delayed compared to the ibandronate solution.

Interestingly, MNP also had a differentiation effect over cells when they did not carry the drug, similar results were previously found [41], and the effect was also delayed to 10 and 15 days as silica Np have to be first available for cells. No significant difference was observed when the two different concentrations of mesoporous silica nanoparticles were incorporated to the culture media. It was recently observed by Ha *et al*., [42] that a bioactive silica-based nanoparticle formulation stimulates *in vitro* differentiation and mineralization of osteoblasts, and increases bone mineral density in young mice *in vivo* demonstrating that these nanoparticles have intrinsic biological activity.

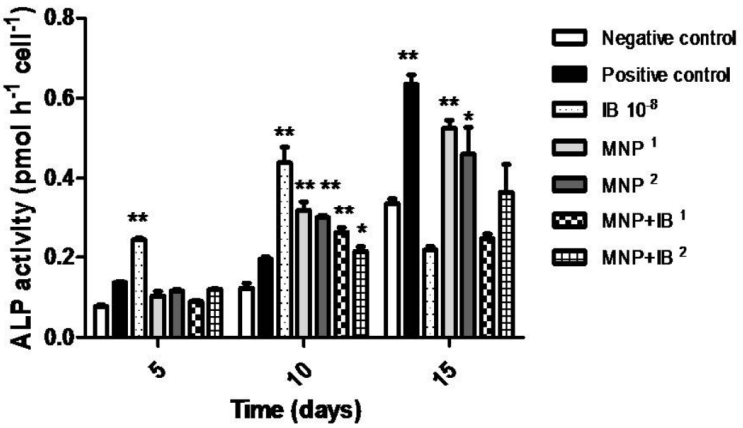


**Fig. (7).** Osteogenic activity of MNP and MNP loaded with sodium ibandronate on mesenchymal cells by measuring the alkaline phosphatase activity of cells. **IB 10 $^{-8}$** indicates a culture media with a content of $10^{-8}$ M sodium ibandronate. **MNP$^{1}$** indicates the presence of 0,36 µg $L^{-1}$ MNP, **MNP$^{2}$** indicates the presence of 3,6 µg $L^{-1}$ MNP, **MNP+ IB$^{1}$** indicates the presence of 0,36 µg $L^{-1}$ MNP loaded with $10^{-8}$ sodium ibandronate and **MNP+ IB$^{2}$** indicates the presence of 3,6 µg $L^{-1}$ MNP loaded with $10^{-7}$ sodium ibandronate. * Indicates a statistical significance compared to the negative control.

In conclusion, these MNP-collagen nanocomposites would represent a valuable alternative for local sustained delivery of bisphosphonates and their potential use as implants for bone regeneration. Indeed, this system combines: i) a well- known inhibitory effect over osteoclasts [4-5] ii) the ability to promote an osteogenic differentiation effect on mesenchymal cells and iii) at the same time they are non toxic for cells. Further *in vivo* studies will be performed.

## CONFLICT OF INTEREST

The author(s) confirm that this article content has no conflict of interest.

## ACKNOWLEDGEMENTS

The authors would like to acknowledge the support of grants from the University of Buenos Aires UBACYT 20020110100081 (to M.F.D) and from Agencia Nacional de Investigaciones Científicas y Técnicas PICT 2012-1441. GSA and MFD are CONICET researchers.

## REFERENCES

[1] Francis, M. The inhibition of calcium hydroxyapatite crystal growth by polyphosphonates and polyphosphates. *Calc. Tis Res.,* **1969**, *3*(1), 151-162.

[2] Russell, R.G.G.; Watts, N.B.; Ebetino, F.H.; Rogers, M.J. Mechanisms of action of bisphosphonates: Similarities and differences and their potential influence on clinical efficacy. *Osteoporos. Int.,* **2008**, *19*(6), 733-759.

[3] Lehenkari, P.P.; Kellinsalmi, M.; Näpänkangas, J.P.; Ylitalo, K.V.; Mönkkönen, J.; Rogers, M.J.; Azhayev, A.; Väänänen, H.K.; Hassinen, I.E. Further insight into mechanism of action of clodronate: Inhibition of mitochondrial ADP/ATP translocase by a nonhydrolyzable, adenine-containing metabolite. *Mol. Pharmacol.,* 2002, *61*(5), 1255-1262.

[4] van Beek, E.; Pieterman, E.; Cohen, L.; Löwik, C.; Papapoulos, S. Farnesyl Pyrophosphate synthase is the molecular target of nitrogen-containing bisphosphonates. *Biochem. Biophys. Res. Commun.,* **1999**, *264*(1), 108-111.

[5] Giger, E.V.; Castagner, B.; Leroux, J.-C. Biomedical applications of bisphosphonates. *J. Control. Release,* **2013**, *167*(2), 175-188.

[6] Ezra, A.; Golomb, G. Administration routes and delivery systems of bisphosphonates for the treatment of bone resorption. *Adv. Drug Del. Rev.,* **2000**, *42*(3), 175-195.

[7] Eberhardt, C.; Habermann, B.; Müller, S.; Schwarz, M.; Bauss, F.; Kurth, A.H. A. The bisphosphonate ibandronate accelerates osseointegration of hydroxyapatite-coated cementless implants in an animal model. *J. Orthop. Sci.,* **2007**, *12*(1), 61-66.

[8] Lalatonne, Y.; Monteil, M.; Jouni, H.; Serfaty, J.M.; Sainte-Catherine, O.; Lièvre, N.; Kusmia, S.; Weinmann, P.; Lecouvey, M.; Motte, L. Superparamagnetic bifunctional bisphosphonates nanoparticles: A potential mri contrast agent for osteoporosis therapy and diagnostic. *J. Osteoporos.,* **2010**, *2010*, **7**.

[9] Salzano, G.; Marra, M.; Porru, M.; Zappavigna, S.; Abbruzzese, A.; La Rotonda, M.I.; Leonetti, C.; Caraglia, M.; De Rosa, G. Self-assembly nanoparticles for the delivery of bisphosphonates into tumors. *Int. J. Pharmaceut.,* **2011**, *403*(1-2), 292-297.

[10] Kolmas, J.; Sobczak, M.; Olędzka, E.; Nałęcz-Jawecki, G.; Dębek, C., Synthesis, characterization and *in vitro* evaluation of new composite bisphosphonate delivery systems. *Int. J. Mol. Sci.,* **2014**, *15*(9), 16831-16847.

[11] Puppi, D.; Piras, A.M.; Chiellini, F.; Chiellini, E.; Martins, A.; Leonor, I.B.; Neves, N.; Reis, R. Optimized electro- and wet-spinning techniques for the production of polymeric fibrous scaffolds loaded with bisphosphonate and hydroxyapatite. *J. Tissue Eng. Regen. Med.,* **2011**, *5*(4), 253-263.

[12] Samdancioglu, S.; Calis, S.; Sumnu, M.; Atilla Hincal, A. Formulation and *in vitro* evaluation of bisphosphonate loaded microspheres for implantation in osteolysis. *Drug Dev. Ind. Pharm.,* **2006**, *32*(4), 473-481.

[13] Kettenberger, U.; Ston, J.; Thein, E.; Procter, P.; Pioletti, D.P. Does locally delivered Zoledronate influence peri-implant bone formation? – Spatio-temporal monitoring of bone remodeling *in vivo*. *Biomaterials,* **2014**, *35*(37), 9995-10006.

[14] Peter, B.; Pioletti, D.P.; Laïb, S.; Bujoli, B.; Pilet, P.; Janvier, P.; Guicheux, J.; Zambelli, P.Y.; Bouler, J.M.; Gauthier, O. Calcium phosphate drug delivery system: influence of local zoledronate release on bone implant osteointegration. *Bone,* **2005**, *36*(1), **5**2-60.

[15] Rayment, E.A.; Dargaville, T.R.; Shooter, G.K.; George, G.A.; Upton, Z. Attenuation of protease activity in chronic wound fluid with bisphosphonate-functionalised hydrogels. *Biomaterials,* **2008**, *29*(12), 1785-1795.

[16] Bae, H.; Chu, H.; Edalat, F.; Cha, J.M.; Sant, S.; Kashyap, A.; Ahari, A. F.; Kwon, C.H.; Nichol, J.W.; Manoucheri, S.; Zamanian, B.; Wang, Y.; Khademhosseini, A. Development of functional biomaterials with micro- and nanoscale technologies for tissue engineering and drug delivery applications. *J. Tissue Engin. Regenerative Med.,* **2014**, *8*(1), 1-14.

[17] Jeffries, E.M.; Wang, Y. Biomimetic micropatterned multi-channel nerve guides by templated electrospinning. *Biotechnol. Bioengin.,* **2012**, *109*(6), 1571-1582.

[18] You, Z.; Bi, X.; Fan, X.; Wang, Y. A functional polymer designed for bone tissue engineering. *Acta Biomaterialia,* **2012**, *8*(2), 502-510.

[19] de Vries-van Melle, M.L.; Tihaya, M.S.; Kops, N.; Koevoet, W.J.L.M.; Mary Murphy, J.; Verhaar, J.A.N.; Alini, M.; Eglin, D.; van Osch, G.J.V.M. Chondrogenic differentiation of human bone marrow-derived mesenchymal stem cells in a simulated osteochondral environment is hydrogel dependent. *Europ. Cells . Mater.,* **2014**, *27*, 112-123.

[20] Johnstone, B.; Alini, M.; Cucchiarini, M.; Dodge, G.R.; Eglin, D.; Guilak, F.; Madry, H.; Mata, A.; Mauck, R.L.; Semino, C.E.; Stoddar, M.J. Tissue engineering for articular cartilage repair - The state of the art. *Europ. Cells Mater.,* **2012**, *25*, 248-267.

[21] Pirvu, T.; Blanquer, S.B.G.; Benneker, L.M.; Grijpma, D.W.; Richards, R.G.; Alini, M.; Eglin, D.; Grad, S.; Li, Z. A combined biomaterial and cellular approach for annulus fibrosus rupture repair. *Biomaterials,* **2015**, *42*, 11-19.

[22] Heinemann, S.; Coradin, T.; Desimone, M.F. Bio-inspired silica-collagen materials: Applications and perspectives in the medical field. *Biomat. Sci.,* **2013**, *1*(7), 688-702.

[23] Desimone, M. F.; Hélary, C.; Mosser, G.; Giraud-Guille, M. M.; Livage, J.; Coradin, T. Fibroblast encapsulation in hybrid silica-collagen hydrogels. *J. Mater. Chem.,* **2010**, *20*(4), 666-668.

[24] Desimone, M.F.; Hélary, C.; Rietveld, I.B.; Bataille, I.; Mosser, G.; Giraud-Guille, M. M.; Livage, J.; Coradin, T. Silica-collagen bionanocomposites as three-dimensional scaffolds for fibroblast immobilization. *Acta Biomaterialia,* **2010**, *6*(10), 3998-4004.

[25] Foglia, M.L.; Camporotondi, D.E.; Alvarez, G.S.; Heinemann, S.; Hanke, T.; Perez, C.J.; Diaz, L.E.; Desimone, M.F. A new method for the preparation of biocompatible silica coated-collagen hydrogels. *J. Mater. Chem. B,* **2013**, *1*(45), 6283-6290.

[26] Quignard, S.; Copello, G. J.; Aimé, C.; Bataille, I.; Hélary, C.; Desimone, M. F.; Coradin, T., Influence of silicification on the structural and biological properties of buffer-mediated collagen hydrogels. *Adv. Engin. Mater.,* **2012**, *14*(3), B51-B55.

[27] Foglia, M.L.; Alvarez, G.S.; Catalano, P.N.; Mebert, A.M.; Diaz, L.E.; Coradin, T.; Desimone, M.F. Recent patents on the synthesis and application of silica nanoparticles for drug delivery. *Rec. Pat. Biotechnol.,* **2011**, *5*(1), 54-61.

[28] Mebert, A.M.; Camporotondi, D.E.; Foglia, M.L.; Alvarez, G.S.; Orihuela, P.L. S.; Diaz, L.E.; Desimone, M.F. Controlling the interaction between cells and silica nanoparticles. *J. Biomat. Tissue Engin.,* **2013**, *3*(1), 108-121.

[29] He, Q.; Shi, J. Mesoporous silica nanoparticle based nano drug delivery systems: Synthesis, controlled drug release and delivery, pharmacokinetics and biocompatibility. *J. Mater. Chem.,* **2011**, *21*(16), 5845-5855.

[30] Wu, K.C.W.; Yamauchi, Y. Controlling physical features of mesoporous silica nanoparticles (MSNs) for emerging applications. *J. Mat. Chem.,* **2012**, *22*(4), 1251-1256.

[31] Stöber, W.; Fink, A.; Bohn, E. Controlled growth of monodisperse silica spheres in the micron size range. *J. Colloid Interface Sci.,* **1968**, *26*(1), 62-69.

[32] Yang, M.; Wang, G.; Yang, Z. Synthesis of hollow spheres with mesoporous silica nanoparticles shell. *Mater. Chem. Phys.,* **2008**, *111*(1), 5-8.

[33] Brunauer, S.; Emmett, P.H.; Teller, E. Adsorption of Gases in Multimolecular Layers. *J. Amer. Chem. Soc.,* **1938**, *60*(2), 309-319.

[34] Barrett, E.P.; Joyner, L.G.; Halenda, P.P. The Determination of Pore Volume and Area Distributions in Porous Substances. I. Computations from Nitrogen Isotherms. *J. Amer. Chem. Soc.,* **1951**, *73*(1), 373-380.

[35] Alvarez, G.S.; Foglia, M. L.; Camporotondi, D.; Giorgeri, S.; Desimone, M. F.; Luis, E.D. Zoledronate and related impurities analysis by capillary zone electrophoresis. *Curr. Anal. Chem.,* **2014**, *10*, 231-234.

[36] Alvarez, G.S.; Helary, C.; Mebert, A.M.; Wang, X.; Coradin, T.; Desimone, M. F. Antibiotic-loaded silica nanoparticle-collagen composite hydrogels with prolonged antimicrobial activity for wound infection prevention. *J. Mater. Chem. B,* **2014**, *2*(29), 4660-4670.

[37] Zhang, L.; Chan, C. Isolation and enrichment of rat mesenchymal stem cells (mscs) and separation of single-colony derived MSCs. *J. Vis. Exp.,* **2010**, (37), 1852.

[38] Valerio, P.; Pereira, M.M.; Goes, A. M.; Leite, M.F. The effect of ionic products from bioactive glass dissolution on osteoblast proliferation and collagen production. *Biomater.,* **2004**, *25*(15), **2941-2948**.

[39] Casado-Díaz, A.; Santiago-Mora, R.; Dorado, G.; Quesada-Gómez, J.M. Risedronate positively affects osteogenic differentiation of human mesenchymal stromal cells. *Arch. Med. Res.,* **2013**, *44*(5), 325-334.

[40] von Knoch, F.; Jaquiery, C.; Kowalsky, M.; Schaeren, S.; Alabre, C.; Martin, I.; Rubash, H.E.; Shanbhag, A.S. Effects of bisphosphonates on proliferation and osteoblast differentiation of human bone marrow stromal cells. *Biomater.,* **2005**, *26*(34), 6941-6949.

[41] Neumann, A.; Christel, A.; Kasper, C.; Behrens, P. BMP2-loaded nanoporous silica nanoparticles promote osteogenic differentiation of human mesenchymal stem cells. *RSC Adv.,* **2013**, *3*(46), 24222-24230.

[42] Ha, S.-W.; Weitzmann, M.N.; Beck, G.R. Bioactive silica nanoparticles promote osteoblast differentiation through stimulation of autophagy and direct association with LC3 and p62. *ACS Nano,* **2014**, *8*(6), 5898-5910.

**Received: January 14, 2015** **Revised: February 19, 2015** **Accepted: March 02, 2015**